British Journal of Cancer

ARTICLE

Check for updates

Cellular and Molecular Biology

# Sec61γ is a vital protein in the endoplasmic reticulum membrane promoting tumor metastasis and invasion in lung adenocarcinoma

Shanqi Xu[1,3], Xin Li[2,3], Jianxiong Geng[1], Yingyue Cao[1], Yan Yu[1]✉ and Lishuang Qi[2]✉



**BACKGROUND:** Lung adenocarcinoma (LUAD) is one of the most common malignant tumors worldwide. Finding effective prognostic markers and therapeutic targets is of great significance for controlling metastasis and invasion clinically.
**METHODS:** The open copy-number aberrations and gene expression datasets were analysed, and the data of 102 LUAD patients was used for further validation. The cell proliferation, colony formation, migration, invasion assays and mice tumor models were used to detect the function of *SEC61G*. The epidermal growth factor receptor (EGFR) pathway was also detected to find the mechanism of Sec61γ.
**RESULTS:** Based on the open datasets, we found that the high level of *SEC61G* mRNA may drive LUAD metastasis. Furthermore, the overexpression of Sec61γ protein was significantly associated with poor prognosis and greater tumor cell proliferation and metastasis. The *SEC61G* knockdown could inhibit the EGFR pathway, including STAT3, AKT and PI3K, which can be reversed by Sec61γ overexpression and epithelial growth factor (EGF) supplement.
**CONCLUSIONS:** Sec61γ promoted the proliferation, metastasis, and invasion of LUAD through EGFR pathways. Sec61γ might be a potential target for the treatment of LUAD metastases.

*British Journal of Cancer* (2023) 128:1478–1490; https://doi.org/10.1038/s41416-023-02150-z

## INTRODUCTION

Lung cancer, a rapidly metastatic and highly invasive cancer, has become the top killer cancer threatening human health and life. It is the most frequently diagnosed cancer, and its mortality ranks first in cancer-induced death, as reported by the Global Cancer Statistics 2018 [1]. On the basis of the histopathological type, lung cancer can be divided into non-small cell lung cancer (NSCLC) and small cell lung cancer (SCLC), among which lung adenocarcinoma (LUAD) is one of the most common subtypes [2]. Although current studies on molecular markers and therapeutic targets for lung cancer are very extensive, limited genes can be used in clinical practice to effectively suppress metastasis and improve prognosis [3]. Thus, finding effective targets for alleviating the proliferation, migration and invasion of lung cancer is of great significance, which would significantly ameliorate the prognosis of patients. However, the false-negative rate of current preoperative imaging techniques in detecting tiny distant metastases would limit the study on tumor metastasis [4, 5]. Previously, we have reported a prognostic signature, including 9 gene pairs (9-GPS), for identifying LUAD patients with potential occult metastases [6, 7], which could aid in the identification of robust genomic characteristics of LUAD patients with metastases.

Proteins expressed in the endoplasmic reticulum (ER) membrane play a significant role in polypeptide translocation into the ER [8]. The translocation channel allows the polypeptide chain to translocate across the ER lumen [9]. In eukaryotes, Sec61, Sec62 and Sec63 are the core proteins comprising the translocation channel [10], and the Sec61 complex achieves its function through interaction with ribosome and membrane protein [11, 12]. The conserved heterotrimeric membrane-protein Sec61 complex constructs the protein-conducting channel for the translocation of a majority proteins [13]. Additionally, the Sec61 complex is reported to be a potential ER $Ca^{2+}$ leak channel associated with cell motility and invasion [14, 15]. To sum up, existing studies demonstrate that Sec61 plays a regulatory role in intracellular signal transduction and protein transport.

Recently, there are few studies on Sec61γ, especially in LUAD. One report utilised *SEC61G* as a latent prognostic marker for predicting survival and treatment response in glioblastoma patients [16]. Another research reported that Sec61γ, one member of the *SEC61* translocon, was obviously upregulated in glioblastoma patients [17]. In NSCLC clinical samples, increased Sec62 expression was noticeably associated with decreased patient survival [18]. Metastasis, a process where tumor cells spread

[1]Department of Medical Oncology, Harbin Medical University Cancer Hospital, Harbin, China. [2]College of Bioinformatics Science and Technology, Harbin Medical University, Harbin, China. [3]These authors contributed equally: Shanqi Xu, Xin Li. ✉email: yuyan@hrbmu.edu.cn; qilishuang7@ems.hrbmu.edu.cn

Received: 16 June 2021 Revised: 1 December 2022 Accepted: 11 January 2023
Published online: 9 February 2023

progressively from the primary site to distant colonising organs, is a main factor of cancer patients' deaths [16]. In NSCLC patients, high levels of Sec62 are correlated with lymph node metastasis and poorly differentiated tumors [19], suggesting its potential function on tumor metastasis. However, the latent roles of these proteins as diagnostic or prognostic biomarkers remain unknown, and the potential correlation between Sec61γ expression and tumor development need to be further studied.

A previous study exhibited that *SEC61G* modulated downstream signalling pathways through acting as an independent gene or a *SEC61G*-epidermal growth factor receptor (*EGFR*) gene fusion [20]. Another study on glioblastoma indicated that *SEC61G* and *EGFR* are frequently co-amplified and co-expressed in the same patient [21]. These results imply that the expression patterns of Sec61γ and EGFR may be interdependent. As is known, EGFR pathway activation could significantly facilitate tumor development and progression. The activated EGFR protein can initiate various downstream signalling pathways, including phosphatidylinositol 3-kinase (PI3K)/protein kinase B (AKT) [22] and STAT3 [23] pathways, which could promote epithelial–mesenchymal transition (EMT) and upregulation matrix metalloproteinases (MMPs) [24, 25]. All these changes can significantly promote tumor growth, metastasis and angiogenesis [26, 27]. In addition, tumor cells can release angiogenesis factors, such as vascular endothelial growth factor (VEGF), to stimulate the growth of neovascularization [28, 29]. A recent study found that the 216G/T-induced overexpression of the EGFR protein was associated with the pleural metastasis risk of LUAD [30].

In this study, we utilised 9-GPS-assisted clinical diagnosis to select the potential molecular markers that are highly expressed in LUAD metastasis samples and remarkably associated with the prognosis. The results demonstrated that Sec61γ might be a key factor on the metastasis, invasion, and clinical prognosis of LUAD. To confirm whether Sec61γ was a potential marker for lung cancer, we identified the function of Sec61γ on metastasis and invasion of LUAD with cell lines and mice. Moreover, the interaction and co-expression of Sec61γ and EGF on related signalling pathways were investigated. We supposed that Sec61γ was a potentially effective tumor marker and therapeutic target ameliorating the proliferation, metastasis and prognosis of LUAD.

## MATERIALS AND METHODS

### Public data and preprocessing

The copy-number aberrations (CNAs) and mRNA expression profiles of 511 Stage I–IV primary LUAD samples were downloaded from The Cancer Genome Atlas (TCGA) database (http://cancergenome.nih.gov/). The LUAD samples included 218 samples of patients without metastases, and 293 samples of patients with lymph node metastases or distal metastases. The other three public gene expression profiles were downloaded from Gene Expression Omnibus (GEO, http://www.ncbi.nlm.nih.gov/geo/), which were used to test the association of gene expressions with cancer progression and metastasis. As described in Table 1, two datasets (GSE68465 and GSE31210) recorded survival information of 315 and 204 Stage I–III LUAD patients without receiving adjuvant therapies, respectively, and one dataset (GSE50081) included 94 samples of patients without metastases and 33 samples of LUAD patients with lymph node metastases.

CNA data derived from TCGA were processed with the GISTIC algorithm using the thresholds of 0.3 for copy-number amplified regions and −0.3 for copy-number deleted regions. For transcriptional data derived from Illumina HiSeq 2000 RNA Sequencing Version 2, the normalised count values processed by RSEM method were extracted and log-transformed ($log_2$(-RSEM + 1)) as the gene expression measurements. For transcriptional data generated by Affymetrix platforms, the Robust Multi-array Average algorithm was used for preprocessing the raw data. Probe IDs were mapped to Gene IDs according to the corresponding platform files. For each sample, the expression measurements of all probes corresponding to the same Gene ID were averaged to obtain a single measurement. Probes that did not match any Gene ID or matched multiple Gene IDs were deleted.

**Table 1.** Correlation between *SEC61G* gene levels and LUAD occurrence and metastasis.

| Characteristic | Data | T state | *P* value |
|---|---|---|---|
| LUAD vs normal | | | |
| | GSE18842 | 6.9944 | 3.25E-09 |
| | GSE19804 | 6.8202 | 4.13E-10 |
| Metastasis vs non-metastasis | | | |
| Pathological metastasis | GSE50081 | 1.4204 | 0.157207 |
| Pathological metastasis +7/9− GPS-assisted | GSE50081 | 4.6771 | 5.71E-06 |
| Pathological metastasis | GSE30219 | 1.1553 | 0.2489 |
| Pathological metastasis +7/9− GPS-assisted | GSE30219 | 5.8223 | 1.56E-08 |

### Reclassification of metastasis states with the aid of prognostic signature

First, the prognostic 9-GPS, consisting of nine gene pairs with a strict voting criterion for low-risk identification [6], was applied to the gene expression profiles of 511 LUAD samples derived from TCGA. A cancer sample was classified as a low-metastasis risk if more than seven gene pairs in 9-GPS (7/9-GPS) voted for low-metastasis risk, and vice versa. The detailed risk classification rule of 7/9-GPS was described in the original literature [6, 7]. Here, patients who were clinical diagnosed as non-metastasis ($N_0M_0$) and classified as a low-metastasis risk by 7/9-GPS were defined as the non-metastasis group, and the other patients who were clinically diagnosed as metastasis or classified as a high-metastasis risk by 7/9-GPS were defined as the metastasis group.

### Clinical sample

Tissue samples were obtained from 102 LUAD patients who underwent surgery at Harbin Medical University Cancer Hospital (Heilongjiang, China) from 2008 to 2014. All experiments were operated under the tenets of the Declaration of Helsinki, and each subject signed informed consent. The clinical data, including age, sex, smoking status, tumor stage, primary tumor size and lymph node status, were recorded.

### Animals and cell lines

Adult female BALB/c nude mice (4–6 weeks) were obtained from the Experimental Animal Center, Chinese Academy of Sciences (Beijing, China). All animal studies were conducted in compliance with the American Animal Protection Legislation and with ethical approval by the Institutional Animal Care and Use Committee of Harbin Medical University. The mice were maintained under a specific pathogen-free environment with 12 h light/dark cycles at 22 °C and 60% relative humidity and were treated with free access to water and food.

Human NSCLC cells (HCC827, H1299, H1650, H1915, A549 and PC9), human large-cell lung carcinoma cells (H460 and H661), human lung squamous carcinoma cells (H2170) and LUAD cells (PC14) were all obtained from the American Type Culture Collection (Manassas, VA, USA). Cells were cultured in DMEM supplemented with FBS (Gibco), 1% L-glutamine (Gibco), and 1% penicillin–streptomycin (Gibco), in an atmosphere of 5% $CO_2$ at 37 °C. A549 and H1650 which were used frequently in this project had been identified the sources by STR profiling.

### Immunohistochemistry staining

Five micrometres of paraffin-embedded tissues was deparaffinized with a xylene soak and rehydrated by decreasing the concentration alcohol. A 95 °C water bath was utilised for antigen retrieval with citrate-based buffer at pH 6.0 for 20 min prior to Sec61γ polyclonal antibody (Proteintech, 11147-2-AP, 1:50) incubation. The tissue samples were treated with biotinylated secondary antibody (Servicebio, GB23303, 1:200), after washing with PBS for three times. Then, slides were treated with avidin-biotin–peroxidase complex, counterstained with haematoxylin, and examined with a light microscope (Olympus, Tokyo, Japan). The Sec61γ intensity was measured with a four-point intensity scale (a): 0-point (no staining), 1-point (faint staining), 2-point (moderate staining), and 3-point (strong staining). The percentage of positive cells (b) was categorised as follows: <1%, score 0; 1–29%, score 1; 30–69%, score 2; and >70%, score 3.

The final score was calculated by (a) × (b): negative (–), score 0; weakly positive (+), score 1–3; positive (++), score 4–6; strongly positive (+++), score 7–9. The samples were divided into the high-Sec61G group (score 4–9) and low-Sec61G group (score 0–3) based on Sec61G expression.

### Immunofluorescence staining

Cells were seeded on the coverslips and were fixed in 4% paraformaldehyde. After being treated with 0.5% Triton X-100 for permeabilization, cells were incubated with Sec61γ primary antibody (Proteintech, 11147-2-AP, 1:50) at 4 °C overnight. After washing with PBS for three times, coverslips were incubated with Cy3-conjugated goat anti-rabbit fluorescent secondary antibody (Servicebio, GB21303, 1:300) for 1 h in the dark at room temperature. After washing with PBS for three times, the coverslips were stained with DAPI (4, 6-diamidino-2-phenylindole, dihydrochloride). Fluorescence images were obtained using 3DHistech Pannoramic SCAN (3DHistech Ltd., Hungary). Six randomly selected fields in each group were photographed (×200 magnification). The mean fluorescence intensity was quantified using Image J software.

### Plasmids construction

For gene silencing or overexpression, we constructed *SEC61G* siRNA-1 and siRNA-2, negative control (NC) siRNA, Lv-sh*SEC61G*, Lv-scramble, *SEC61G* overexpression vector or NC vector based on the procedure. The siRNA sequences are: siRNA-1: 5′-CACTAAACCTGATAGAAAA-3′; siRNA-2: 5′-GACTCCATTCGGCTGGTTA-3′.

siRNA sequences for Lv-scramble are: TTCTCCGAACGTGTCACGTAA,

shRNA sequences for Lv-shSec61G are:

GATCCGTTCTCCGAACGTGTCACGTAATTCAAGAGATTACGTGACACGTTCG GAGAATTTTTTC (Top strand),

AATTGAAAAAATTCTCCGAACGTGTCACGTAATCTCTTGAATTACGTGACAC GTTCGGAGAACG (Bottom strand).

qRT-PCR was utilised to evaluate the silencing or overexpression effect.

### Virus transfection

Before lentivirus transfection, cell paving was operated, and cells were planted in 12-well plates ($1.2 \times 10^5$ cells /well) or in six-well plates ($2.4 \times 10^5$ cells/well). The next day, the original culture medium was removed with 2 mL fresh culture medium, including polybrene (6 g/mL). The viral suspension was added and cells were cultured under 37 °C for 4 h. Lipofectamine 2000 reagent (Beyotime, Shanghai, China) was used for virus transfection. Then, the medium was changed, and the incubation continued for 24 h. After that, the medium containing virus was substituted by fresh medium. After 24–48 h, subsequent experiments were operated.

### qRT-PCR

RNA was extracted with Trizol reagent (Invitrogen, Carlsbad, CA, USA) as stated by the description. The cDNA was produced by the FastQuant RT kit (Tiangen, Beijing, China) in accordance with the procedure. The *SEC61G* level was analysed with Talent qPCR PreMix (SYBR Green) (Tiangen, Beijing, China) in an ABI prism 7500 sequence detection system. The statistics were standardised with β-actin. The primer sequences used in this study are:

Sec61g F: 5′-ATGGGATTCATTGGCTTCTTTG-3′,
Sec61g R: 5′-TTTCTCACACCCTCACACTTG-3′;
β-actin F: 5′-TCGTGCGTGACATTAAGGAGAAG-3′,
β-actin R: 5′-GTTGAAGGTAGTTTCGTGGATGC-3′.

### Western blot

The tissues were cut into sections and prepared with RIPA buffer, including protease inhibitors, followed by centrifugation. Then the protein concentration was detected with BCA protein assay kit (Tiangen, Beijing, China). After that, equal amounts of proteins were separated with electrophoresis in SDS-PAGE (8–15% separating gel and 5% stacking gel). Then they were removed onto PVDF membranes and blocked with 5% non-fat milk powder for 1 h. Subsequently, at 4 °C, they were incubated overnight with primary antibodies of anti-EGFR (Rayantibody, RM6002, 1:3000), anti-p-EGFR (Bioss, BS-5317R, 1:2000), anti-AKT (Abcam, ab8805, 1:1000), anti-p-AKT (Immunoway, YP0006, 1:2000), anti-PI3K (Abcam, ab189403, 1:1000), anti-p-PI3K (Abcam, ab182651, 1:1000), anti-STAT3 (Abcam, ab119352, 1:5000), anti-p-STAT3 (Cell Signaling, 4113, 1:2000), anti-β-actin (Rayantibody, RM2001, 1:2500), and Sec61γ (Proteintech, 11147-2-AP, 1:200), followed by washing with TBST. Then, they were incubated at room temperature for 1 h with corresponding secondary antibodies. Finally, blots were developed with enhanced ECL Plus reagent (Millipore, Billerica, MA, USA).

### CCK-8 assay

CCK-8 (Beyotime, Shanghai, China) was utilised for the detection of Cell proliferation. The cells with or without transfection were collected at a density of $1–2 \times 10^5$ cells/well and added into 96-well plates (100 μL/well). After that, they were added with CCK-8 (10 μL/well) at various time points (0, 1, 2 and 3 d) and incubated for 3 h at 37 °C. Finally, a microplate reader (Molecular Devices, California, USA) was applied to detect the absorbance of each well at 450 nm to analyse the viable cell number.

### Colony-formation assay

Cells were seeded into 6-well plates with 600 cells/well. During 2 weeks of incubation, the culture medium was replaced every 3 days. When visible colonies appeared, the incubation was terminated. After fixation with by 4% paraformaldehyde, the cells were stained by 0.1% crystal violet (Amresco, Solon, OH, USA). The colonies were photographed and counted.

### Wound-healing assay

Cells were seeded into six-well plates and incubated until 70% confluence. Then, they were scratched with a 200 μL pipette tip to create a linear wound. Afterwards, the cells were washed three times with warmed PBS to remove cell debris and floating cells. Then, they were cultured with serum-free medium and incubated under 37 °C with 5% $CO_2$. At specified time points (0 and 24 or 48 h) after the scratch, images were taken by a microscope system (Olympus, Tokyo, Japan). Five wound positions were randomly selected for measurement in each group. The wound-healing rate was calculated as follows: wound-healing rate (%) = (0-h width – 24-h width)/0-h width × 100%.

### Transwell migration assay

The migratory potential of cells was analysed with transwell inserts (Corning Incorporated, Corning NY, USA). Briefly, 600 μL of serum-free DMEM culture medium was added into the bottom chamber, and 200 μL was added into the upper chamber. The culture medium was balanced in the transwell inserts for 1 h at 37 °C before being removed. After 12-h starvation, 200 μL of cell suspension was added to the upper chamber. Cells were accessible to migrate to the bottom chamber placed with complete medium including 10% FBS in advance. After 24 or 48 h, culture media were removed, and cells were washed with PBS twice. After fixation with 4% paraformaldehyde, 0.1% crystal violet (Amresco, Solon, OH, USA) was applied for staining cells for 15 min. The observation of cell migration was captured by an inverted microscope system (Olympus, Tokyo, Japan). Three visual fields were randomly selected.

### Transwell invasion assay

After the addition of serum-free DMEM culture medium as described in the transwell migration assay above, transwell inserts (Corning Incorporated, Corning NY, USA) were coated with 100 μL of Matrigel (BD Biosciences, Franklin Lakes, NJ, USA) and placed in an incubator overnight at 37 °C. Then, 200 μL of cell suspension was added into the upper chamber, whereas culture medium (700 μL) including 10% FBS was added into the bottom chamber, and incubated for 24 or 48 h at 37 °C. After fixation with 4% paraformaldehyde, 0.1% crystal violet (Amresco, Solon, OH, USA) was used to stain the cells that invaded the bottom chamber. Finally, the invaded cells were visualised and calculated using the inverted microscope system (Olympus, Tokyo, Japan). Three visual fields were randomly selected.

### Animal model of metastasis and in vivo imaging system

A549 cells were cultured in RMPI1640 containing 10% FBS under 37 °C and suspended in a serum-free medium during their logarithmic growth phase. Eight mice were randomly divided into two groups, four mice per group. About 100 μL of suspended cells ($1 \times 10^7$/mL) was administered into the BALB/c nude mice by tail vein injection. After 4 weeks, the mice were administrated with luciferin substrate (Promega, Madison, WI, USA) via intraperitoneal injection and the region of the lung was quantified with small animal imaging system (IVIS, Caliper, Newton, MA, USA).

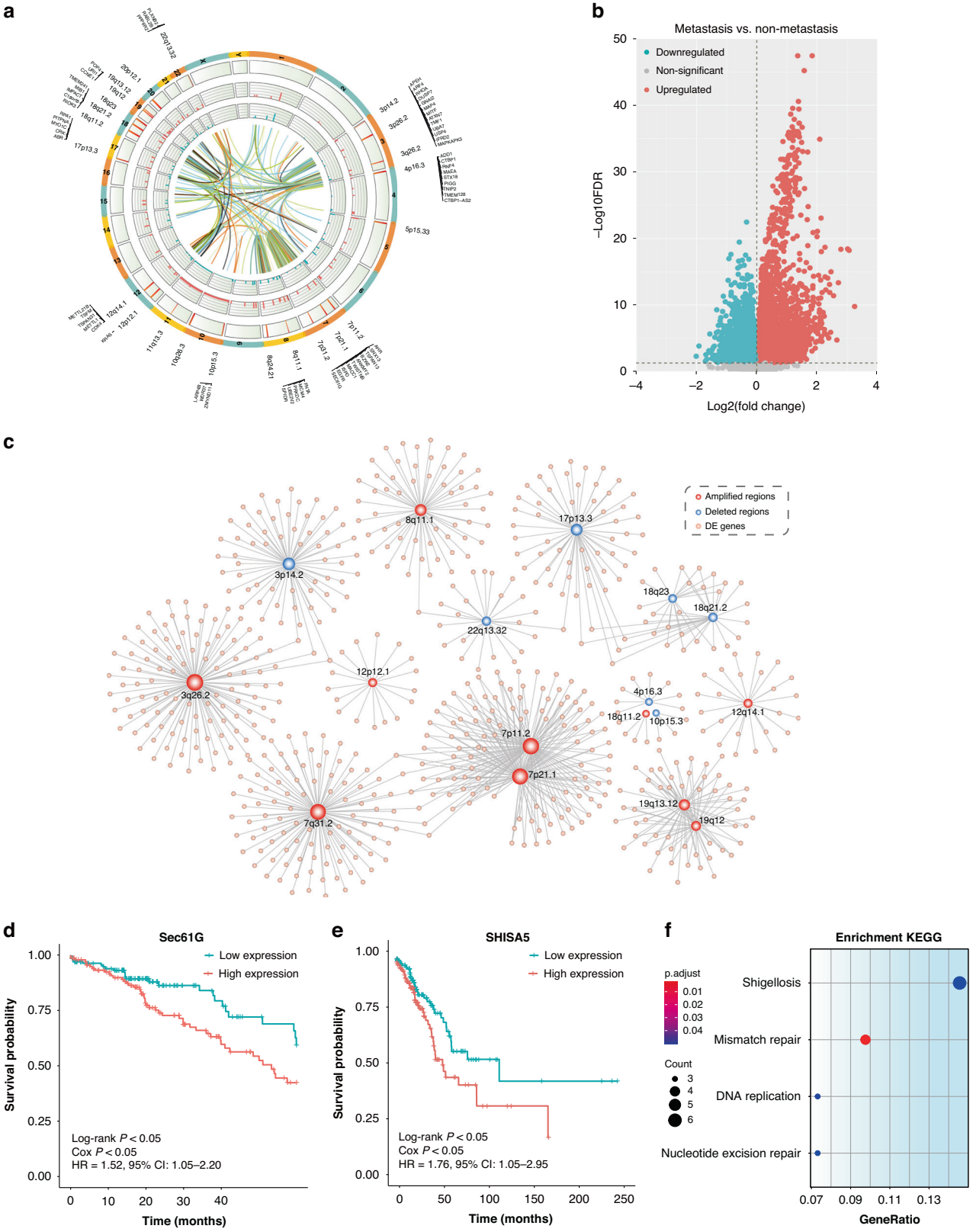


## Statistical analysis

Fisher's exact test was used to identify the copy regions that had significantly different CNA frequencies between the two groups. Student's *t* test was performed to extract significantly differentially expressed (DE) genes between two groups. Spearman's rank correlation was used to estimate the correlation between the CNA regions and the gene expressions. The cluster Profiler package in R software [31] was used to perform functional enrichment analysis of interesting genes based on the Kyoto Encyclopedia of Genes and Genomes (KEGG) database, and illustrated by Cluster Profiler and ggplot2 package in R (Wickham H: ggplot2: Elegant Graphics for Data Analysis. Springer-Verlag, https://doi.org/10.1080/15366367.2019.1565254).

**Fig. 1 Identification of oncogenes for LUAD metastasis in TCGA data. a** Circos diagram of metastasis-related CNA regions. The first ring (outermost) shows the genomic regions of 23 potential metastasis-related CNAs (red vertical bar), whose alterations had significantly higher frequencies in the reclassified metastasis group than in the reclassified non-metastasis group with the aid of 7/9-GPS. Here, some of the genes, whose expression levels were significantly related with their own CNAs, are demonstrated. The second and third rings show histograms of the frequencies of metastasis-related CNAs in the reclassified metastasis group and the non-metastasis group, respectively. The center of the Circos plot shows the relationship between these CNAs and mRNA levels of 643 metastasis-related DE genes, whose expressions were significantly different between the reclassified metastasis and non-metastasis groups. **b** Volcano plot of metastasis-related DE genes. **c** Regulatory network of metastasis-related CNAs. The regulatory network includes 17 potential metastasis-related CNAs, consisting of 46 amplified genes and 112 deleted genes, linked with 643 metastasis-related DE genes. Three metastasis-related CNAs, 3q26.2, 7p11.2 and 7p21.1, regulate the most metastasis-related DE genes. **d, e** Kaplan–Meier curves of OS for patients according to the mRNA level of *SEC61G* (**d**) and *SHISA5* (**e**). HR and 95% CI were generated using univariate Cox regression models. **f** Functional pathways enriched with the metastasis-related DE genes regulated by *SEC61G* in the network. The enrichment analysis was performed by cluster Profiler package in R software based on the KEGG database.

The overall survival (OS) was defined as the time from surgery to death or the final documented date (censored). The survival curve was estimated using the Kaplan–Meier method and compared using the log-rank test [32] The univariate Cox proportional-hazards regression model was used to evaluate the association of the gene expressions with OS. Hazard ratios (HRs) and 95% confidence intervals (CIs) were generated using the Cox proportional-hazards model.

Statistical comparisons between groups were analysed by ANOVA for data from cells and mice to evaluate the significance. The *P* values were adjusted using the Benjamini–Hochberg procedure for multiple testing to control the false discovery rate (FDR) [33]. All statistical analyses for bioinformatics were performed using R 3.6.1 (http://www.r-project.org/). Data from cells and mice were statistically analysed with SPSS version 21.0. These data were presented as mean ± SD obtained from three independent experiments. The significance was defined as $P < 0.05$ or FDR < 0.05 for multiple testing.

## RESULTS

### *SEC61G* is an oncogene for LUAD metastasis

Our previous report had shown that the reclassification of metastasis states of LUAD patients with the aid of 7/9-GPS could capture more metastasis-related genomic alterations by reducing the influence of samples with occult metastases. In this study, we first applied 7/9-GPS to the gene expression profiles of LUAD derived from The Cancer Genome Atlas (TCGA) database to reclassify the metastasis status of patients, and identified 23 genomic regions that had significantly different frequencies of copy-number aberrations (CNAs) between the redefined metastasis and redefined non-metastasis groups (Fisher's exact test, FDR < 0.05, Fig. 1a). Notably, all 23 genomic alterations had significantly higher frequencies of CNAs in the reclassified metastasis group than in the reclassified non-metastasis group, which were defined as metastasis-related CNAs. Spearman's rank correlation analysis showed that 158 genes located in 17 metastasis-related CNAs regions were positively correlated with their own CNAs (Spearman's rank correlation, FDR < 0.05, Fig. 1a). Then, using Student's *t* test with 5% FDR control, we found 8358 differentially expressed (DE) genes between the reclassified metastases and non-metastases group (Fig. 1b). Spearman's rank correlation was used to estimate the correlation between the metastasis-related CNAs regions and metastasis-related DE genes. Finally, we constructed a regulator network by linking the 17 metastasis-related CNVs regions, comprising 46 amplified genes and 112 deleted genes, with 643 metastasis-related DE genes (Fig. 1c). As shown in Fig. 1c, three metastasis-related CNV regions (3q26.2, 7p11.2 and 7p21.1) appeared to regulate the most metastasis-related DE genes in the network. The other metastasis-related CNV regions could also regulate the metastasis-related DE genes.

Furthermore, we performed survival analyses for 158 genes in the 17 metastasis-related CNV regions and found that the overexpression of two genes (*SEC61G* located on 7p11.2 and *SHISA5* located on 3p14.2) was significantly associated with poor patient OS by the log-rank test and univariate Cox analysis (*SEC61G*: log-rank $P < 0.05$, cox $P < 0.05$, HR = 1.52, 95% CI: 1.05–2.20, Fig. 1d; *SHISA5*: log-rank $P < 0.05$, cox $P < 0.05$, HR = 1.76, 95% CI: 1.05–2.95, Fig. 1e). The results of survival analyses for all 158 genes are displayed in Supplementary Table S1. Notably, *SEC61G* located on 7p11.2 region, could regulate 106 metastasis-related DE genes in the network, and these genes were significantly enriched in "Mismatch repair", "DNA replication", "Nucleotide excision repair" and "Shigellosis" signalling pathways (hypergeometric distribution model, FDR < 0.05, Fig. 1f). The above results suggested that the overexpressed *SEC61G*, caused by its amplification, might drive the metastasis of LUAD patients. The prognostic performance of *SEC61G* mRNA transcription was validated in GSE68465 (log-rank $P < 0.05$, cox $P < 0.05$, HR = 1.65, 95% CI = 1.29–2.11, Fig. 2a) and GSE31210 (log-rank $P < 0.05$, cox <0.05, HR = 1.66, 95% CI = 1.07–2.57, Fig. 2b). Importantly, the mRNA of *SEC61G* was significantly differentially expressed between the two metastasis groups reclassified by 7/9-GPS in the GSE50081 dataset (Student's *t* test, $P < 0.01$, Fig. 2c).

### Sec61γ was correlated with the progression, metastasis and prognosis of lung cancer with clinical samples

To further confirm the relationship between Sec61γ protein expression and LUAD, LUAD tissues ($n = 102$) were collected from the clinic. They were separated into two groups (i.e., high expression group and low expression group) (Fig. 2d), according to Sec61γ level detected by immunohistochemical (IHC) staining. Afterwards, an analysis of the pathological characteristics and survival analysis were carried out. The results showed that in high-Sec61γ group the proportion of cases at Stages II and III and primary tumor size (T3/T4) was significantly increased in the high-Sec61γ group ($P < 0.05$) (Table 2). Meanwhile, in high-Sec61γ group the proportion of moderately poorly differentiated samples was obviously decreased in the high-Sec61γ group ($P < 0.01$) (Table 2). The survival analyses showed that the patients in the high-Sec61γ group had significantly shorter OS than those in the low-Sec61γ group ($P < 0.05$, Fig. 2e).

### Sec61γ promoted lung cancer cells proliferation

To confirm suitable lung cancer cell lines for exploring the function and mechanism of *SEC61G*, the original expression of *SEC61G* mRNA level in 10 cell lines (H460, H661, HCC827, H1299, H1650, H1915, H2170, A549, PC9 and PC14) were detected by qRT-PCR method (Fig. 3a, b). We ultimately selected the A549 cell line with high level of *SEC61G* transcription background and H1650 cell line with low level of *SEC61G* transcription background for the follow-up experiments. To confirm the specificity of Sec61γ antibody, a *SEC61G* overexpression (OE) vector and its negative control (NC) vector (empty vector) were constructed. The immunofluorescent (IF) staining of Sec61γ was performed in H1650 cells, which were transfected with *SEC61G* OE vector and NC vector, respectively. We observed visible higher fluorescence intensity in the *SEC61G* overexpression (OE) group than in the negative control (NC) group (Fig. 3c). To observe the impact of Sec61γ on the proliferation, migration and invasion of lung cancer cells, the *SEC61G* overexpression vector was constructed to

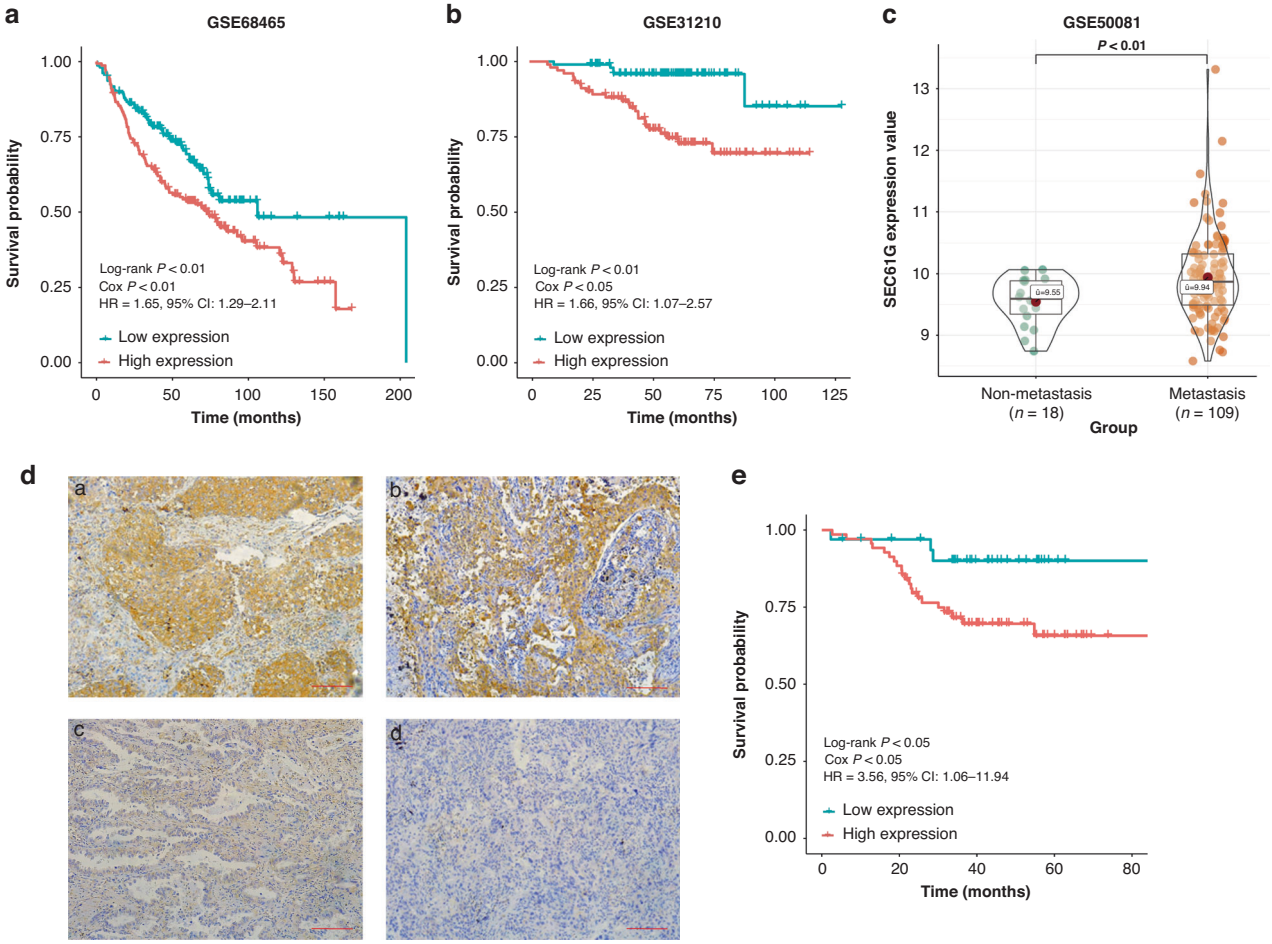


**Fig. 2 Survival analysis of different Sec61γ expressions in LUAD patients from different resources.** The Kaplan–Meier curves of overall survival (OS) for patients according to mRNA level of *SEC61G* in the GSE68465 public dataset (**a**) and in the GSE31210 public dataset (**b**). **c** The violin plot of the *SEC61G* mRNA level between the reclassified metastasis and reclassified non-metastasis groups with the aid of 7/9-GPS in the GSE50081 public dataset. **d** Immunohistochemistry analysis of Sec61γ in LUAD tissue. Strong staining was considered as high expression (**a**). Moderate staining was considered as high expression (**b**). Weak staining was considered as low expression (**c**). Negative staining was considered as low expression (**d**). **e** The Kaplan–Meier curves of overall survival (OS) for patients according to the protein level of Sec61γ.

increase SEC61γ levels in H1650 cells, and two candidate siRNAs were constructed to decrease Sec61γ levels in A549 cells, NC siRNA was constructed as a negative control. The mRNA and protein expressions of Sec61γ presented a significant increase in the overexpression (OE) group in H1650 cells ($P < 0.05$) (Fig. 3d, f). Compared with the negative control (NC) group, the mRNA and protein expressions of Sec61γ were considerably decreased in siRNA-1 and siRNA-2 groups in A549 cells ($P < 0.05$) (Fig. 3e, g), then siRNA-1 was utilised for subsequent functional research. CCK-8 assay was applied to explore the effect of Sec61γ on proliferation. The results showed that the $OD_{450}$ of the over-expression group was remarkably increased, compared with the NC group in H1650 cells ($P < 0.01$) (Fig. 3h). In Sec61γ knockdown A549 cells, we observed significantly lower $OD_{450}$ from the 1st day ($P < 0.01$) (Fig. 3l). To investigate the impact of Sec61γ on lung cells colony-forming ability, colony-formation assay was performed. We observed the upregulation of colony-forming ability in the Sec61γ overexpression group in H1650 cells ($P < 0.01$) (Fig. 3j, l) and the downregulation of colony-forming ability in the Sec61γ knock-down group in A549 cells ($P < 0.01$) (Fig. 3k, m).

### Sec61γ enhanced the migration and invasion of lung cancer cells

To explore the impact of Sec61γ on lung cancer migration, wound-healing assay was performed. The data presented that the wound-healing rate of the Sec61γ overexpression group was remarkably higher than that of the NC group ($P < 0.01$) at 48 h in H1650 cells (Fig. 4a, c). In A549 cells, the wound-healing rate was lower in the Sec61γ knockdown group compared with the NC group at 24 h ($P < 0.01$) (Fig. 4b, d). The results showed that Sec61γ enhanced the metastasis of lung cancer cells. Consistently, the transwell assay manifested that the overexpression and suppression of Sec61γ could enhance and inhibit the migration, respectively ($P < 0.01$) (Fig. 4e–h).

To explore the impact of Sec61γ on invasion, a transwell invasion assay was performed to assess the ability to penetrate the matrix glue. The statistics demonstrated that the number of cells penetrating matrix glue was significantly increased in the overexpression group of H1650 cells ($P < 0.01$) (Fig. 4i, k) and decreased in the knockdown group of A549 cells ($P < 0.01$) (Fig. 4j, l), compared with the corresponding NC group. These results indicated that Sec61γ could enhance the invasiveness of lung cancer cells.

### Effect of Sec61γ on the metastasis of cancer cells in mice

To further confirm the impact of Sec61G on metastasis in vivo, Lv-sh*SEC61G* was constructed to interfere Sec61γ expression in A549 cells. qRT-PCR verified that *SEC61G* was downregulated by Lv-sh*SEC61G* ($P < 0.01$) (Fig. 5a), suggesting that *SEC61G* knockdown was successfully achieved in A549 cells. Then these A549 cells

**Table 2.** Correlation between Sec61γ expression level and clinicopathological characteristics in LUAD.

| Clinical characteristics | Total number | Sec61γ-high cases | Sec61γ-low cases | *P* value |
|---|---|---|---|---|
| Age (years) | | | | 0.544 |
| <60 | 60 | 42 | 18 | |
| ≥60 | 42 | 27 | 15 | |
| Sex | | | | 0.618 |
| Female | 50 | 35 | 15 | |
| Male | 52 | 34 | 18 | |
| Smoking status | | | | 0.960 |
| Smoker | 46 | 31 | 15 | |
| Non-smoker | 56 | 38 | 18 | |
| Tumor stage | | | | 0.034* |
| I | 39 | 21 | 18 | |
| II | 47 | 34 | 13 | |
| III | 16 | 14 | 2 | |
| Primary tumor size | | | | 0.049* |
| T1 | 39 | 21 | 18 | |
| T2 | 50 | 37 | 13 | |
| T3-4 | 13 | 11 | 2 | |
| Lymph node status | | | | 0.058 |
| Negative | 42 | 24 | 18 | |
| Positive | 60 | 45 | 15 | |
| Differentiation | | | | 0.001** |
| Well-differentiated | 25 | 10 | 15 | |
| Moderately poorly | 77 | 59 | 18 | |

Note: Sec61γ-high vs Sec61γ-low: *$P < 0.05$; **$P < 0.01$.

were injected into mice via the tail vein. Data presented that the bioluminescence intensity was lower in Lv-sh*SEC61G* mice than in Lv-scramble mice detected by in vivo imaging system ($P < 0.01$) (Fig. 5b, c), suggesting the inhibition effect on lung metastasis via Sec61γ knockdown.

### Sec61γ regulated the EGFR signalling pathway in lung cancer cells

A previous study reported a novel *SEC61G-EGFR* fusion gene in paediatric ependymomas [20], indicating that Sec61γ might participate in the EGFR pathway. Therefore, we further explored the association of *SEC61G* and *EGFR* mRNA transcription in TCGA, and found a significant association between the two genes (Pearson correlation, $r = 0.24$, $P < 0.01$, Fig. 6a), suggesting that Sec61G might promote LUAD metastases by regulating the EGFR signalling pathway. Therefore, we detected the protein expressions of p-EGFR/EGFR, p-AKT/AKT, p-PI3K/PI3K and p-STAT3/STAT3 in A549 cells. After Sec61γ was knockdown (KD) by Lv-sh*SEC61G*, the levels of p-EGFR, p-AKT, p-PI3K and p-STAT3 were evidently decreased ($P < 0.05$) (Fig. 6b). Furthermore, EGF was added into A549 cells. We found that in EGF (+) cells, the phosphorylated and non-phosphorylated protein levels of AKT, PI3K and STAT3 in the KD group and NC group were remarkably elevated compared with the corresponding groups of EGF (−) cells ($P < 0.05$) (Fig. 6b). Meanwhile, the expressions of the above factors in the KD group were noticeably lower than those in the NC group, both in EGF (+) cells and EGF (–) cells ($P < 0.05$) (Fig. 6b). On the contrary, Sec61γ overexpression could active EGFR signalling pathway in H1650 cells (Fig. 6c). However, EGFR inhibitor gefitinib could significantly inhibit Sec61γ function. The levels of p-EGFR, p-AKT, p-PI3K and p-STAT3 were significantly decreased even though high level of Sec61γ still existed (Fig. 6d). These data suggested that Sec61γ might modulate the development of lung cancer through the EGFR signalling pathway.

## DISCUSSION

Lung cancer is the leading factor in cancer-related deaths in terms of morbidity and mortality worldwide, and the most common histopathological subtype is adenocarcinoma [34]. Tumor metastasis is closely related to poor prognosis in LUAD [35], highlighting that there is an urgent necessity to investigate effective strategies for these cancer patients. Consequently, recognition of novel biomarkers is particularly meaningful for the early detection and targeted molecular therapies of lung cancer [3, 36]. In this research, we identified and verified that Sec61γ expression level was correlated with the metastasis and prognosis of LUAD in public data and clinical samples. The overexpression of Sec61γ protein was demonstrated to enhance cell proliferation, clone formation, metastasis and invasion. Moreover, Sec61γ regulated EGFR and its downstream pathways through a non-competitive manner with EGF. As far as we know, prior to this study, the function of Sec61γ in tumorigenesis and metastasis remained largely uninvestigated, especially in lung cancer. Our findings imply a considerable therapeutic value of targeting Sec61γ in fighting cancer progression.

The Sec61 complex, located in the ER membrane, plays an important function in the transport of precursor polypeptides [37]. Recent studies have reported that Sec61 channel also serves as a passive calcium leak channel of ER [38], revealing an additional function of Secs in intracellular signalling transmission. The Sec61 complex is composed of three subunits, Sec61α, β and γ, which together form a channel [39–41]. Sec61α forms the actual channel, while Sec61β and Sec61γ are attached the channel on the periphery, and connected to the lipid bilayer [42]. The relationship between Sec61α, Sec61β and cancer is rarely reported. Sec61α has been indicated to facilitate cell proliferation, migration and stemness in hepatocellular carcinoma [43]. Sec61β is involved in the dislocation of EGFR and hepatocyte growth factor receptor (c-

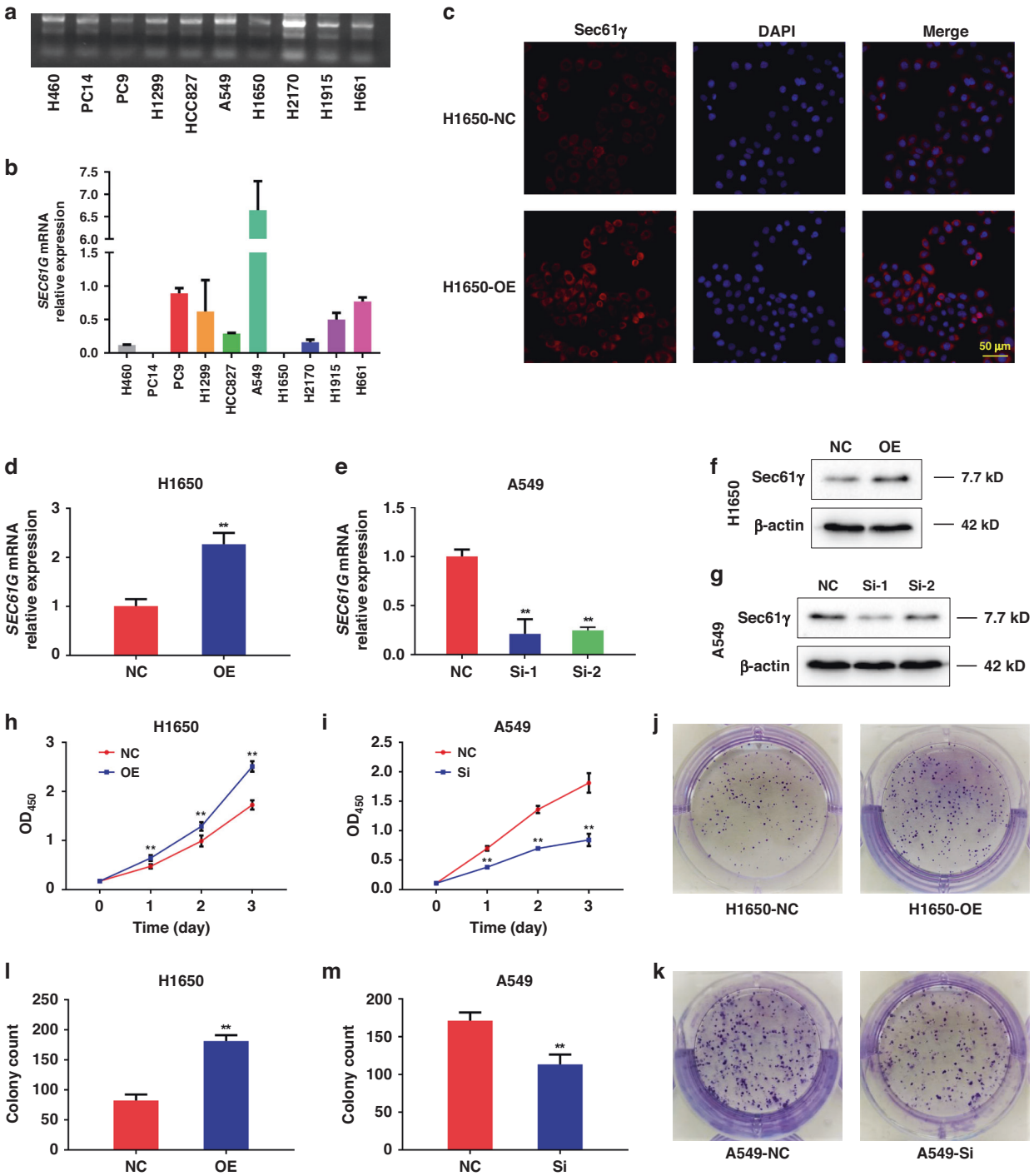


**Fig. 3 Effects of Sec61γ on the proliferation of lung cell lines. a** Agarose gel electrophoretogram of total RNA extracted in different cell lines. **b** qRT-PCR results of *SEC61G* mRNA relative expression in different lung cell lines. **c** Immunofluorescence staining results of overexpression of Sec61γ protein in 1650 cell line. **d** qRT-PCR results of overexpression of *SEC61G* mRNA in H1650 cell line. **e** qRT-PCR results of knockdown of *SEC61G* mRNA in A549 cell line. **f** Western blot results of overexpression of Sec61γ protein in H1650 cell line. **g** Western blot results of knockdown of Sec61γ protein in A549. **h** Overexpression of Sec61γ on proliferation in H1650 cell line. **i** Knockdown of Sec61γ on proliferation in A549 cell line. **j**–**m** Effects of Sec61γ regulation on colony formation in lung cell lines. **j** Overexpression of Sec61γ in H1650 cell line and colony formation in H1650-NC and H1650-OE groups. **k** Knockdown of Sec61γ in A549 cell line and colony formation in A549-NC and A549-Si groups. **l** Statistical results of H1650 colony count. **m** Statistical results of A549 colony count. Data were presented as mean ± SD. $n = 6$. $^{*}P < 0.05$, $^{**}P < 0.01$. NC negative control group, OE overexpression group, Si siRNA group.

MET) [44, 45], implying that Sec61β has the potential to regulate cell proliferation. Sec61γ, which is known as Sec61 translocon subunit-γ, is the main member of the Sec61 complex [39, 40]. Currently, along with its high frequency of gene amplification, Sec61γ is significantly upregulated in a majority of glioblastoma multiforme cases, and knockdown Sec61γ expression leads to growth suppression and apoptosis in tumor cells [17]. Additionally, Sec62 and Sec63 have been found to be potential markers of

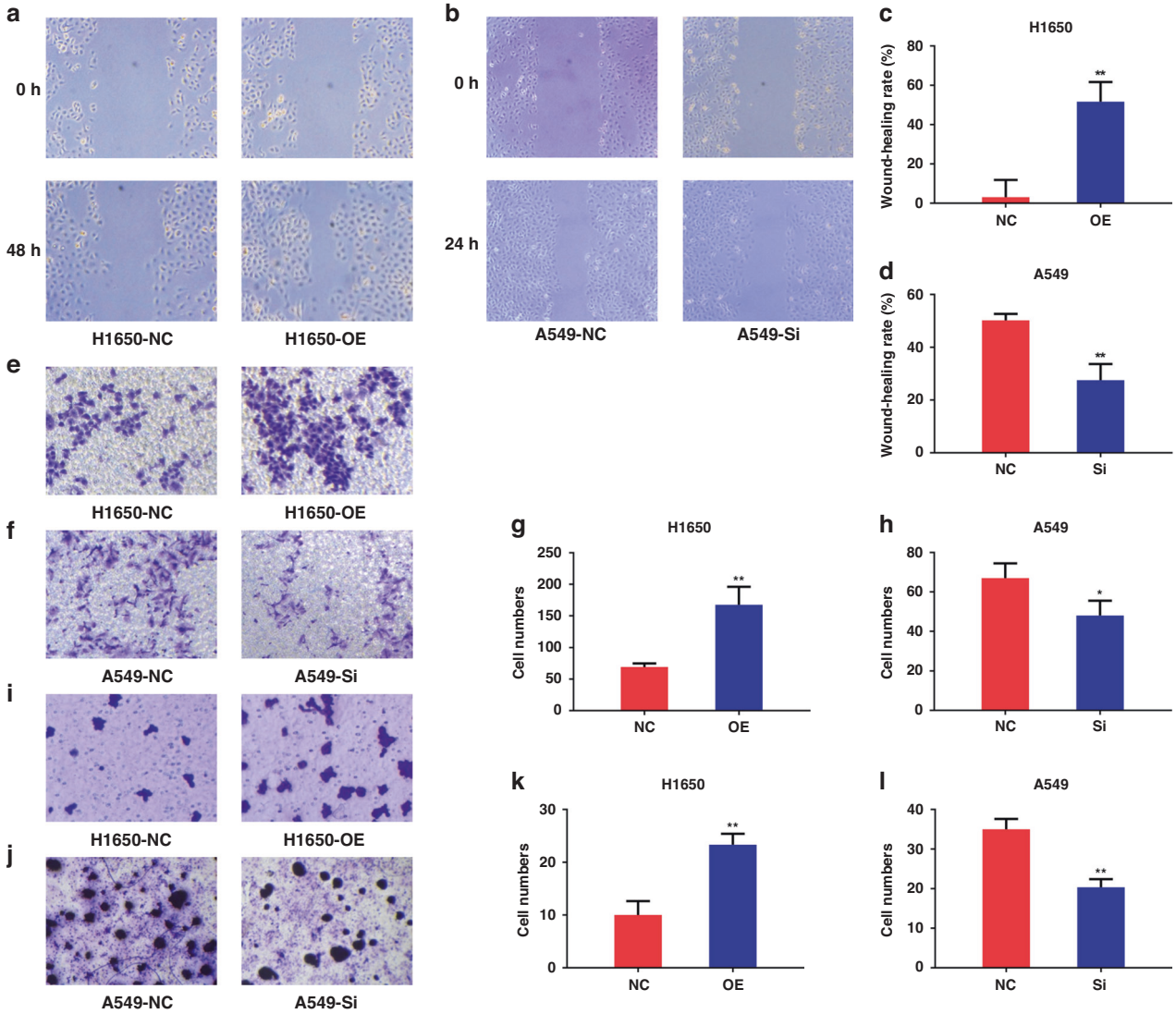


**Fig. 4 Sec61γ enhanced the migration and invasion of lung cancer cells. a–d** Effects of Sec61γ regulation on lung cell lines in a wound-healing assay. **a** Overexpression of Sec61γ in H1650 cell line and wound-healing results in H1650-NC and H1650-OE groups at 0 or 48 h. **b** Knockdown of Sec61γ in A549 cell line and wound-healing results in A549-NC and A549-Si groups at 0 or 24 h. **c** Statistical results of H1650 cell wound-healing rate. **d** Statistical results of A549 cell wound-healing rate. **e** Overexpression of Sec61γ in H1650 cell line and transwell migration in H1650-NC and H1650-OE groups. **f** Knockdown of Sec61γ in A549 cell line and transwell migration in A549-NC and A549-Si groups. **g** Statistical results of H1650 cell transwell assay. **h** Statistical results of A549 cell transwell assay. **i–l** Transwell invasion results of Sec61γ regulation in lung cell lines. **i** Overexpression of Sec61γ in H1650 cell line and transwell invasion in H1650-NC and H1650-OE groups. **j** Knockdown of Sec61γ in A549 cell line and transwell invasion in A549-NC and A549-Si groups. **k** Statistical results of H1650 cell invasion test. **l** Statistical results of A549 cell invasion test. Data were presented as mean ± SD. $n = 6$. $^{**}P < 0.01$.

gastric, prostate, colorectal cancers and hepatocellular carcinoma [38, 46, 47]. Sec62 overproduction is significantly correlated with poor patient survival in lung cancer [18]. However, the function of Sec61γ in cancer remains to be elucidated. Our results demonstrated that Sec61γ expression was associated with tumor stage, primary tumor size, and differentiation degree in LUAD patients. In the survival analysis, the disease-free survival and OS in the high-Sec61γ group were lower in LUAD patients. To our knowledge, this study is the first to document the relationship between Sec61γ and lung cancer, emphasising a critical role of Sec61γ in metastasis and prognosis of LUAD in the clinic.

Numerous studies have shown that inhibiting the proliferation, metastasis and invasion of lung cancer contributes to improved prognosis [48, 49]. We found that H1650 cells with Sec61γ overexpression exhibited a promotion effect on proliferation, colony formation, migration and invasion in cells, whereas A549 cells with Sec61γ knockdown presented decreased malignant degree. Consistent with the in vitro observation, mouse xenograft models exhibited that tumor formation was significantly suppressed in the lung when A549 cells with Sec61γ knockdown were intravenously delivered into mice. Our results revealed that Sec61γ modulated the proliferation, migration, and invasion of lung cancer. We basically confirmed the oncogenic effects of Sec61γ on the growth and development of lung cancer. A previous study has validated that Sec62 is overproduced in different tumors, most considerably in the prostate, lung and thyroid tumors, whereas cell migration and invasion potential are prevented or at least significantly decreased after Sec62 silencing [50]. Sec62 expression was upregulated in gastric cancer cells, and Sec62 depletion prevented the proliferation and promoted the apoptosis of these cancer cells [16]. Lung and thyroid cancer cells exhibit noticeable migration inhibition in Sec62-depleted cells and migration

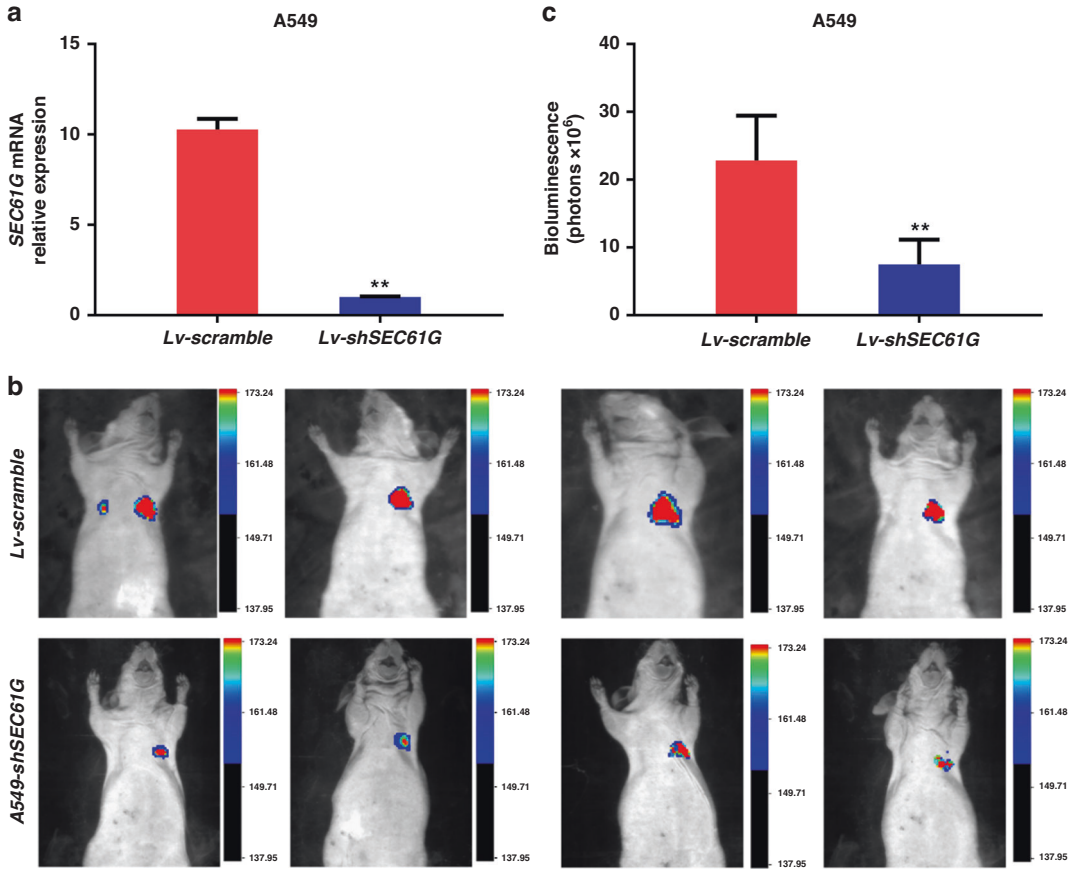


**Fig. 5 Effects of Sec61γ on the metastatic ability of lung cancer cell lines in vivo. a** qRT-PCR verification after *SEC61G* knockdown in A549 cell lines. **b** Small animal imaging. **c** Statistical results of bioluminescence intensity. Data were presented as mean ± SD. $n = 6$. $^{*}P < 0.05$, $^{**}P < 0.01$.

promotion in Sec62-overexpressing cells [19]. Low expression of Sec63 in hepatocellular carcinoma was significantly correlated with an increased proliferative activity and decreased apoptosis [51]. Consistent with previous studies regarding the oncogenic roles of Sec62 and Sec63, we proposed that Sec61γ exerts tumor-promotion functions in lung cancer. In our study, high-Sec61γ expression indicates the enhanced malignant degree of lung cancer, implying that targeting Sec61γ may be an innovative prospect for developing new anticancer reagents to fight metastatic cancers.

EGFR is a receptor for the proliferation and signalling of epithelial growth factor (EGF) cells, also known as HER1 or ErbB1, and its mutation or overexpression is generally associated with tumor occurrence [52]. EGFR has become a vital therapeutic target for NSCLC treatment, and inhibitors targeting the EGFR kinase domain have been established and are widely being used in the clinic [53]. Tyrosine kinase inhibitors (TKIs) represent a crucial pillar in the treatment of lung cancer, which directs at sensitising mutations of the EGFR gene [54]. Two EGFR mutants (ΔN566 and ΔN599) were recognised as products of intrachromosomal rearrangements, fusing the 3′ coding portion of the EGFR gene to the 5′-UTR of the *SEC61G*, and *SEC61G*-EGFR chimeric mRNAs was recognised in one infratentorial ependymoma WHO III [20], indicating that *SEC61G* might regulate downstream signalling pathways by acting as an independent gene or *SEC61G-EGFR* fusion gene. In this research, we observed that Sec61γ could activate EGFR pathway and upregulate the expression of p-AKT/AKT, p-PI3K/PI3K and STAT3. Moreover, the simultaneous upregulation of Sec61γ and EGF obviously stimulated EGFR and its downstream factors. At the time of diagnosis and follow-up after curative resection, a considerable association was found between EGFR mutation and brain metastases risk in pulmonary adenocarcinoma [55], indicating the distinct clinical features of EGFR-mutated tumors in terms of brain metastases. In other words, our discoveries demonstrate the importance of the interaction between Sec61γ and tumorigenesis and metastasis of lung cancer, showing that Sec61γ exerts oncogenic function in lung cancer cells at least partly through the EGFR pathway. Sec61γ may also cooperate with EGF to regulate the progression of lung cancer; however, the accurate regulatory mechanism between Sec61γ and EGFR pathway remains to be further studied. In addition, we estimated the correlation of mRNA level of *SEC61G* with some important molecular characteristics (Supplementary Material 1). *SEC61G* expression was significantly positively correlated with hypoxia [56] and stemness scores [57], but significantly negatively correlated with immune scores [58] (Pearson correlation, $P < 0.0001$). Previous studies have reported that *SEC61G* could promote metastasis via modulating glycolysis and epithelial–mesenchymal transition in breast cancer [59], and *SEC61G* was associated with resistance to apoptosis in kidney cancer [60]. Therefore, the association of Sec61γ activity with other signalling pathways in LUAD merits further exploration.

In summary, our results strongly indicate a key role of Sec61γ in the progression, metastasis and prognosis of LUAD, as verified by data from bioinformatics and clinical samples. In vivo and in vitro, Sec61γ apparently promotes the proliferation, metastasis and invasion of lung cancer, which may modulate the development of lung cancer through the EGFR signalling pathway. The present study provides crucial insight

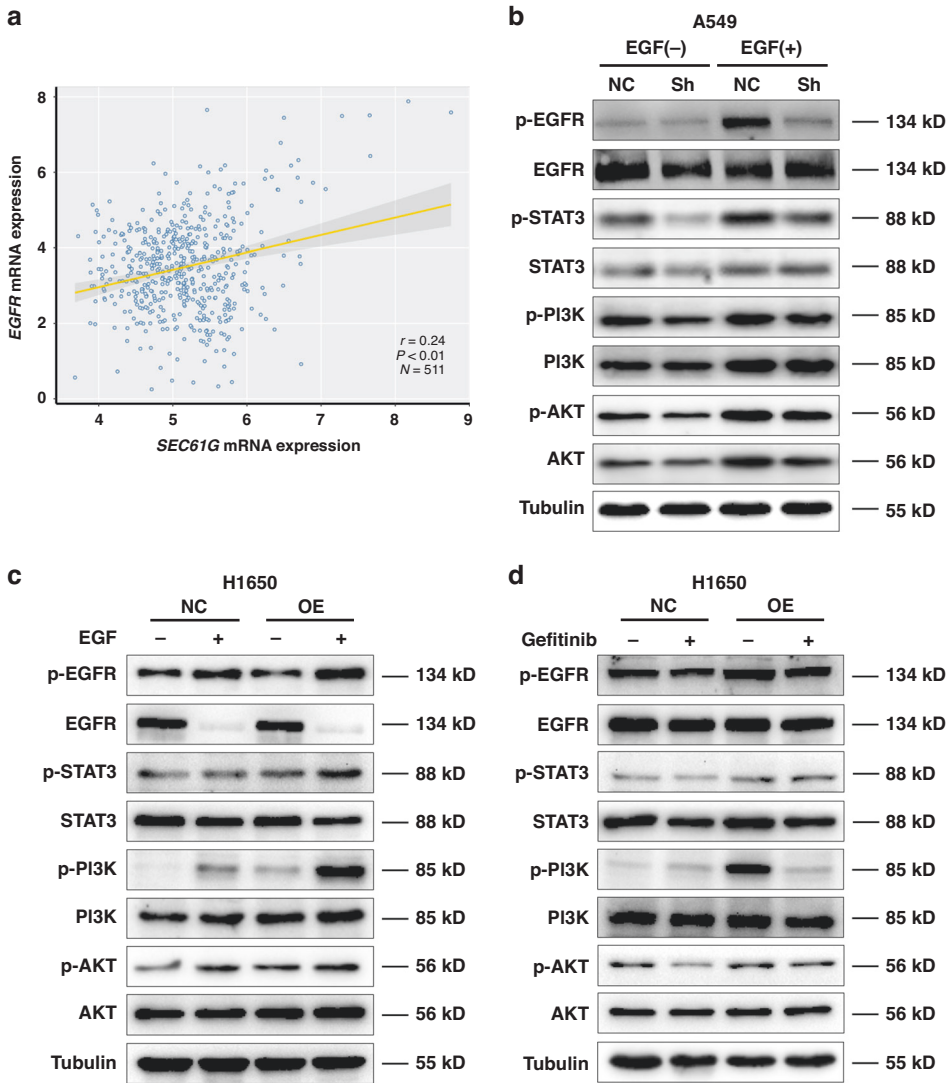


**Fig. 6 Sec61γ regulated the EGFR pathway through related factors. a** Correlation of *SEC61G* with *EGFR* in TCGA mRNA expression data. **b**–**d** Effects of Sec61γ regulation on the activity of EGFR and EGFR pathway-related factors. **b** EGF treatment in A549 cell line. **c** EGF treatment in H1650 cell line. **d** Gefitinib treatment in H1650 cell line.

into understanding the functions of Sec61γ in lung cancer and suggests that targeting Sec61γ may be a novel therapeutic approach for lung cancer treatment.

## DATA AVAILABILITY

The data and material presented in this article and in the Supplementary Information are available from the corresponding authors on reasonable request.

## REFERENCES

1. Bray F, Ferlay J, Soerjomataram I, Siegel RL, Torre LA, Jemal A. Global cancer statistics 2018: GLOBOCAN estimates of incidence and mortality worldwide for 36 cancers in 185 countries. CA Cancer J Clin. 2018;68:394–424.
2. O'Brien TD, Jia P, Caporaso NE, Landi MT, Zhao Z. Weak sharing of genetic association signals in three lung cancer subtypes: evidence at the SNP, gene, regulation, and pathway levels. Genome Med. 2018;10:16.
3. Seijo LM, Peled N, Ajona D, Boeri M, Field JK, Sozzi G, et al. Biomarkers in lung cancer screening: achievements, promises, and challenges. J Thorac Oncol. 2019;14:343–57.
4. Pieterman RM, van Putten JW, Meuzelaar JJ, Mooyaart EL, Vaalburg W, Koeter GH, et al. Preoperative staging of non-small-cell lung cancer with positron-emission tomography. N Engl J Med. 2000;343:254–61.
5. Li M, Hong G, Cheng J, Li J, Cai H, Li X, et al. Identifying reproducible molecular biomarkers for gastric cancer metastasis with the aid of recurrence information. Sci Rep. 2016;6:24869.
6. Qi L, Li T, Shi G, Wang J, Li X, Zhang S, et al. An individualized gene expression signature for prediction of lung adenocarcinoma metastases. Mol Oncol. 2017;11:1630–45.
7. Qi L, Chen L, Li Y, Qin Y, Pan R, Zhao W, et al. Critical limitations of prognostic signatures based on risk scores summarized from gene expression levels: a case study for resected stage I non-small-cell lung cancer. Brief Bioinform. 2016;17:233–42.
8. Aviram N, Schuldiner M. Targeting and translocation of proteins to the endoplasmic reticulum at a glance. J Cell Sci. 2017;130:4079–85.
9. Rapoport TA, Li L, Park E. Structural and mechanistic insights into protein translocation. Annu Rev Cell Dev Biol. 2017;33:369–90.
10. Tyedmers J, Lerner M, Bies C, Dudek J, Skowronek MH, Haas IG, et al. Homologs of the yeast Sec complex subunits Sec62p and Sec63p are abundant proteins in dog pancreas microsomes. Proc Natl Acad Sci USA. 2000;97:7214–9.
11. Beckmann R, Bubeck D, Grassucci R, Penczek P, Verschoor A, Blobel G, et al. Alignment of conduits for the nascent polypeptide chain in the ribosome-Sec61 complex. Science. 1997;278:2123–6.
12. Rapoport TA, Rolls MM, Jungnickel B. Approaching the mechanism of protein transport across the ER membrane. Curr Opin Cell Biol. 1996;8:499–504.
13. Rapoport TA. Protein translocation across the eukaryotic endoplasmic reticulum and bacterial plasma membranes. Nature. 2007;450:663–9.

14. Schorr S, Klein MC, Gamayun I, Melnyk A, Jung M, Schauble N, et al. Co-chaperone specificity in gating of the polypeptide conducting channel in the membrane of the human endoplasmic reticulum. J Biol Chem. 2015;290:18621–35.
15. Huang JB, Kindzelskii AL, Clark AJ, Petty HR. Identification of channels promoting calcium spikes and waves in HT1080 tumor cells: their apparent roles in cell motility and invasion. Cancer Res. 2004;64:2482–9.
16. Liu B, Liu J, Liao Y, Jin C, Zhang Z, Zhao J, et al. Identification of SEC61G as a novel prognostic marker for predicting survival and response to therapies in patients with glioblastoma. Med Sci Monit. 2019;25:3624–35.
17. Lu Z, Zhou L, Killela P, Rasheed AB, Di C, Poe WE, et al. Glioblastoma proto-oncogene SEC61gamma is required for tumor cell survival and response to endoplasmic reticulum stress. Cancer Res. 2009;69:9105–11.
18. Linxweiler M, Schorr S, Schauble N, Jung M, Linxweiler J, Langer F, et al. Targeting cell migration and the endoplasmic reticulum stress response with calmodulin antagonists: a clinically tested small molecule phenocopy of SEC62 gene silencing in human tumor cells. BMC Cancer. 2013;13:574.
19. Linxweiler M, Linxweiler J, Barth M, Benedix J, Jung V, Kim YJ, et al. Sec62 bridges the gap from 3q amplification to molecular cell biology in non-small cell lung cancer. Am J Pathol. 2012;180:473–83.
20. Servidei T, Meco D, Muto V, Bruselles A, Ciolfi A, Trivieri N, et al. Novel SEC61G-EGFR fusion gene in pediatric ependymomas discovered by clonal expansion of stem cells in absence of exogenous mitogens. Cancer Res. 2017;77:5860–72.
21. Huang Q, Wang K, Wanggou S, Tian J, Li X. A novel co-targeting strategy of EGFR/SEC61G for multi-modality fluorescence/MR/photoacoustic imaging of glioblastoma. Nanomedicine. 2022;40:102509.
22. Zhang B, Zhang Y, Jiang X, Su H, Wang Q, Wudu M, et al. JMJD8 promotes malignant progression of lung cancer by maintaining EGFR stability and EGFR/PI3K/AKT pathway activation. J Cancer. 2021;12:976–87.
23. Akca H, Tani M, Hishida T, Matsumoto S, Yokota J. Activation of the AKT and STAT3 pathways and prolonged survival by a mutant EGFR in human lung cancer cells. Lung Cancer. 2006;54:25–33.
24. Lin LL, Yang F, Zhang DH, Hu C, Yang S, Chen XQ. ARHGAP10 inhibits the epithelial-mesenchymal transition of non-small cell lung cancer by inactivating PI3K/Akt/GSK3beta signaling pathway. Cancer Cell Int. 2021;21:320.
25. Wang S, Yan Y, Cheng Z, Hu Y, Liu T. Sotetsuflavone suppresses invasion and metastasis in non-small-cell lung cancer A549 cells by reversing EMT via the TNF-alpha/NF-kappaB and PI3K/AKT signaling pathway. Cell Death Discov. 2018;4:26.
26. Guan X. Cancer metastases: challenges and opportunities. Acta Pharm Sin B. 2015;5:402–18.
27. Merchant N, Nagaraju GP, Rajitha B, Lammata S, Jella KK, Buchwald ZS, et al. Matrix metalloproteinases: their functional role in lung cancer. Carcinogenesis. 2017;38:766–80.
28. Frezzetti D, Gallo M, Maiello MR, D'Alessio A, Esposito C, Chicchinelli N, et al. VEGF as a potential target in lung cancer. Expert Opin Ther Targets. 2017;21:959–66.
29. Niethammer AG, Xiang R, Becker JC, Wodrich H, Pertl U, Karsten G, et al. A DNA vaccine against VEGF receptor 2 prevents effective angiogenesis and inhibits tumor growth. Nat Med. 2002;8:1369–75.
30. Guo H, Xing Y, Liu R, Chen S, Bian X, Wang F, et al. -216G/T (rs712829), a functional variant of the EGFR promoter, is associated with the pleural metastasis of lung adenocarcinoma. Oncol Lett. 2013;6:693–8.
31. Gao H, Niu W, He Z, Gao C, Peng C, Niu J. SEC61G plays an oncogenic role in hepatocellular carcinoma cells. Cell Cycle. 2020;19:3348–61.
32. Bland JM, Altman DG. The logrank test. BMJ. 2004;328:1073.
33. Klipper-Aurbach Y, Wasserman M, Braunspiegel-Weintrob N, Borstein D, Peleg S, Assa S, et al. Mathematical formulae for the prediction of the residual beta cell function during the first two years of disease in children and adolescents with insulin-dependent diabetes mellitus. Med Hypotheses. 1995;45:486–90.
34. Denisenko TV, Budkevich IN, Zhivotovsky B. Cell death-based treatment of lung adenocarcinoma. Cell Death Dis. 2018;9:117.
35. Rami-Porta R, Call S, Dooms C, Obiols C, Sanchez M, Travis WD, et al. Lung cancer staging: a concise update. Eur Respir J. 2018;51:1800190.
36. Duffy MJ, O'Byrne K. Tissue and blood biomarkers in lung cancer: a review. Adv Clin Chem. 2018;86:1–21.
37. Nguyen D, Stutz R, Schorr S, Lang S, Pfeffer S, Freeze HH, et al. Proteomics reveals signal peptide features determining the client specificity in human TRAP-dependent ER protein import. Nat Commun. 2018;9:3765.
38. Linxweiler M, Schick B, Zimmermann R. Let's talk about Secs: Sec61, Sec62 and Sec63 in signal transduction, oncology and personalized medicine. Signal Transduct Target Ther. 2017;2:17002.
39. Zheng Q, Wang Z, Zhang M, Yu Y, Chen R, Lu T, et al. Prognostic value of SEC61G in lung adenocarcinoma: a comprehensive study based on bioinformatics and in vitro validation. BMC Cancer. 2021;21:1216.
40. Lu T, Chen Y, Gong X, Guo Q, Lin C, Luo Q, et al. SEC61G overexpression and DNA amplification correlates with prognosis and immune cell infiltration in head and neck squamous cell carcinoma. Cancer Med. 2021;10:7847–62.
41. Shah P, Chaumet A, Royle SJ, Bard FA. The NAE pathway: autobahn to the nucleus for cell surface receptors. Cells. 2019;8:915.
42. Kelkar A, Dobberstein B. Sec61beta, a subunit of the Sec61 protein translocation channel at the endoplasmic reticulum, is involved in the transport of Gurken to the plasma membrane. BMC Cell Biol. 2009;10:11.
43. Fa X, Song P, Fu Y, Deng Y, Liu K. Long non-coding RNA VPS9D1-AS1 facilitates cell proliferation, migration and stemness in hepatocellular carcinoma. Cancer Cell Int. 2021;21:131.
44. Wang YN, Yamaguchi H, Huo L, Du Y, Lee HJ, Lee HH, et al. The translocon Sec61beta localized in the inner nuclear membrane transports membrane-embedded EGF receptor to the nucleus. J Biol Chem. 2010;285:38720–9.
45. Chen MK, Du Y, Sun L, Hsu JL, Wang YH, Gao Y, et al. H2O2 induces nuclear transport of the receptor tyrosine kinase c-MET in breast cancer cells via a membrane-bound retrograde trafficking mechanism. J Biol Chem. 2019;294:8516–28.
46. Jung V, Kindich R, Kamradt J, Jung M, Muller M, Schulz WA, et al. Genomic and expression analysis of the 3q25-q26 amplification unit reveals TLOC1/SEC62 as a probable target gene in prostate cancer. Mol Cancer Res. 2006;4:169–76.
47. Yu G, Wang LG, Han Y, He QY. clusterProfiler: an R package for comparing biological themes among gene clusters. OMICS. 2012;16:284–7.
48. Wang Y, Fu M, Liu J, Yang Y, Yu Y, Li J, et al. Inhibition of tumor metastasis by targeted daunorubicin and dioscin codelivery liposomes modified with PFV for the treatment of non-small-cell lung cancer. Int J Nanomed. 2019;14:4071–90.
49. Bremnes RM, Veve R, Hirsch FR, Franklin WA. The E-cadherin cell-cell adhesion complex and lung cancer invasion, metastasis, and prognosis. Lung Cancer. 2002;36:115–24.
50. Greiner M, Kreutzer B, Jung V, Grobholz R, Hasenfus A, Stohr RF, et al. Silencing of the SEC62 gene inhibits migratory and invasive potential of various tumor cells. Int J Cancer. 2011;128:2284–95.
51. Casper M, Weber SN, Kloor M, Mullenbach R, Grobholz R, Lammert F, et al. Hepatocellular carcinoma as extracolonic manifestation of Lynch syndrome indicates SEC63 as potential target gene in hepatocarcinogenesis. Scand J Gastroenterol. 2013;48:344–51.
52. Appert-Collin A, Hubert P, Cremel G, Bennasroune A. Role of ErbB receptors in cancer cell migration and invasion. Front Pharm. 2015;6:283.
53. da Cunha Santos G, Shepherd FA, Tsao MS. EGFR mutations and lung cancer. Annu Rev Pathol. 2011;6:49–69.
54. Lim SM, Syn NL, Cho BC, Soo RA. Acquired resistance to EGFR targeted therapy in non-small cell lung cancer: mechanisms and therapeutic strategies. Cancer Treat Rev. 2018;65:1–10.
55. Shin DY, Na II, Kim CH, Park S, Baek H, Yang SH. EGFR mutation and brain metastasis in pulmonary adenocarcinomas. J Thorac Oncol. 2014;9:195–9.
56. Eustace A, Mani N, Span PN, Irlam JJ, Taylor J, Betts GN, et al. A 26-gene hypoxia signature predicts benefit from hypoxia-modifying therapy in laryngeal cancer but not bladder cancer. Clin Cancer Res. 2013;19:4879–88.
57. Miranda A, Hamilton PT, Zhang AW, Pattnaik S, Becht E, Mezheyeuski A, et al. Cancer stemness, intratumoral heterogeneity, and immune response across cancers. Proc Natl Acad Sci USA. 2019;116:9020–9.
58. Yoshihara K, Shahmoradgoli M, Martinez E, Vegesna R, Kim H, Torres-Garcia W, et al. Inferring tumour purity and stromal and immune cell admixture from expression data. Nat Commun. 2013;4:2612.
59. Ma J, He Z, Zhang H, Zhang W, Gao S, Ni X. SEC61G promotes breast cancer development and metastasis via modulating glycolysis and is transcriptionally regulated by E2F1. Cell Death Dis. 2021;12:550.
60. Meng H, Jiang X, Wang J, Sang Z, Guo L, Yin G, et al. SEC61G is upregulated and required for tumor progression in human kidney cancer. Mol Med Rep. 2021;23:427.

## ACKNOWLEDGEMENTS

The bioinformatics-related results shown here regarding lung adenocarcinoma are based upon data derived from The Cancer Genome Atlas (TCGA) database (http://cancergenome.nih.gov/) and Gene Expression Omnibus (GEO, http://www.ncbi.nlm.nih.gov/geo/), accession number GSE68465, GSE31210 and GSE50081.

## AUTHOR CONTRIBUTIONS

SQX designed and performed the in vitro experiments and statistical analyses, collected clinical samples and performed IHC staining of Sec61γ in these tissues, and drafted and revised the manuscript. XL performed the Bioinformatics research and wrote and revised the manuscript. JXG performed the in vitro experiment. YYC performed the in vivo experiment and statistical analyses. LSQ and YY contributed to study design and supervision. All authors approved the final version of the paper and provided their consent for publication.

## FUNDING

This research was supported by the National Natural Science Foundation of China (grant numbers: 81872396, 81572824 and 81672931).

## COMPETING INTERESTS

The authors declare no competing interests.

## ETHICS APPROVAL AND CONSENT TO PARTICIPATE

Informed consent was obtained from all subjects. The study was conducted in accordance with the Declaration of Helsinki and the International Ethical Guidelines for Biomedical Research. All the clinical and animal experimental protocols in this study were reviewed and approved by the Ethics Committee of the Harbin Medical University Cancer Hospital.

## CONSENT TO PUBLISH

Not applicable.

## ADDITIONAL INFORMATION

**Supplementary information** The online version contains supplementary material available at https://doi.org/10.1038/s41416-023-02150-z.

**Correspondence** and requests for materials should be addressed to Yan Yu or Lishuang Qi.